euronoise

Multimode evaluation of cement behind steel pipe

Benoit Froelich

Etudes et Productions Schlumberger, 1, rue Becquerel, BP 202, 92142 Clamart, France
bfroelich@clamart.oilfield.slb.com

In the context of oilfield well, it is important to evaluate the quality of the cement sheath that fills the annular region between the steel casing and the rock formation. This assessment is performed by combining two ultrasonic techniques using the casing thickness resonance mode and flexural mode. This paper presents the flexural mode dispersion and attenuation curves, and their variations with cement acoustical properties. It is found that attenuation increases linearly with the cement impedance up to a critical value. The high attenuation associated with this critical value provides maximum sensitivity for the most needed intermediate impedances. The critical value corresponds to switching from one flexural mode branch to another branch. Above the critical value, the attenuation drops and eventually reaches very low values for high impedance cement. However, in this case, introducing a slip boundary condition between casing and cement drastically increases the attenuation level. All these effects can be observed on simulated and field waveforms, and help in the interpretation of the annulus condition.

1 Introduction

Ultrasonic imaging is used in fluid filled oil wells in order to assess the steel casing integrity and to evaluate the material filling the annulus between the casing and the rock formation. Cement is pumped in this annulus, and holds the casing in place, protects the casing from corrosive formation fluids and most importantly prevents hydraulic communication between different fluid-bearing layers, and between these layers and surface.

To ascertain whether or not cement has displaced the mud and filled the annulus was first carried out with a pulse-echo ultrasonic technique [1] working at normal incidence. The broadband pulse (250-600 kHz) excites the casing thickness resonance mode, and the analysis of the reflected signal allows for extracting the casing thickness and the acoustic impedance of the material present in the annulus. This acoustic impedance discriminates solid cement from liquid drilling mud left behind, while casing thickness reduction points to pipe wear or corrosion. The lateral resolution of the ultrasonic beam and its associated measurements is 25 mm, and the mechanical azimuthal rotation and vertical displacement of the transducer provides a full coverage of the inner pipe surface. Results are displayed as images for an easy interpretation of the potential problems.

This technique however has some limitations: First, its depth of investigation in the radial direction is limited to the region immediately behind the casing and does not probe the full annulus. Secondly, increasingly utilized lightweight cements exhibit lower acoustic impedance which is harder to differentiate from mud impedance. Recently, a new ultrasonic technique has been introduced [2, 3] to address these issues and complement the results obtained with the thickness resonance mode. This technique brings to benefits the casing flexural mode: Due to the property of its group velocity within a specific frequency range, it allows to perform an enhanced evaluation of the annulus acoustic impedance, and also to provide information on the full annulus depth. In this article, we describe the main characteristics of the mode, first when the steel layer is embedded in fluids, then when cement is present on one side of the layer. The effect of the cement mechanical properties, and of the boundary condition between steel and cement will be investigated.

2 Flexural mode with fluid

The dispersion and attenuation curves for a steel plate 8 mm thick and embedded in water is plotted on Fig.1 in the frequency range 0 to 500 kHz. These curves are the result of a mode search performed with the commercially available code DISPERSE [4]. Although several modes coexist in this frequency range, the plot is restricted to the first antisymmetric flexural mode.

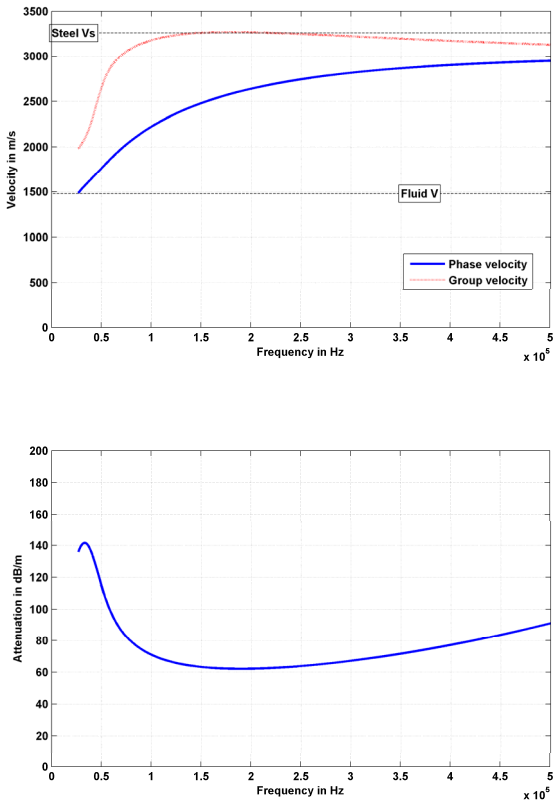

Fig.1 Dispersion and attenuation of a 8 mm steel plate embedded in water

The phase velocity exhibits a large variation, starting at the fluid velocity at low frequency and increasing toward the leaky Rayleigh velocity around 3000 m/s at high frequency.

However, in the same frequency range, the group velocity goes through a broad maximum close to the steel shear velocity, and its value changes by less than 3% between 100 and 400 kHz. This specific feature is at the foundation of the new technique: A compact, broad band ultrasonic pulse propagating along the casing as a flexural mode remains compact, although its wave shape exhibits significant changes due to the dispersive phase velocity. This compactness allows for an easy pulse detection and measurement of its attenuation based on the pulse envelope using multiple receivers. In the same frequency range, the attenuation is largely independent of frequency, making the measurement insensitive to the exact pulse frequency content.

To generate and detect such a flexural wave packet with non contacting transducers, a pitch catch configuration is used (Fig.2). A transmitter launches a short broad band pulse centered at 250 kHz, in the fluid. The transducer angle with respect to the normal to the casing is set according to Snell's law, using the fluid velocity and the flexural phase velocity (2650 m/s at 250 kHz). This angle is typically 33 deg, although it may change according to the fluid and the casing thickness. The wave traveling in the fluid is partly converted into the flexural wave packet, which then propagates along the casing. This propagation takes place with radiation losses, both inside and outside the casing. The receiver transducers, oriented with the same angle as the transmitter, are picking the signals radiated inward. Their spacing is appropriately chosen at 10 cm so that the flexural mode attenuation can be accurately measured by taking the ratio of the echoes envelope peaks. The signal radiated outward in the annulus may eventually be reflected at the annulus to formation interface, goes through the casing with little loss in amplitude, and reaches the receivers, after the main casing arrival. Because pulse compactness is maintained all along, these formation arrivals can easily be separated from the casing arrival for typical annulus thicknesses (20 mm). The difference between their time of arrival and the casing time of arrival provides a measurement of the annulus thickness and geometry or the annulus ultrasonic velocity if the thickness is known by other means

At the frequency of operation, the flexural wavelength is short enough to ensure a lateral resolution of the order of 25 mm, similar to the thickness mode technique. The vertical resolution for the attenuation measurement is controlled by the inter receiver spacing (10 cm). Such a resolution is still much smaller than the defects typically encountered during cementing operations, and which are preferentially elongated in the vertical direction. To provide full coverage of the pipe wall, the set of 3 flexural transducers are actually combined with a normal incidence transducer on a rotating assembly which is translated in the vertical direction. The results from both independent modes are combined to provide an enhanced answer to the actual state of the annulus material.

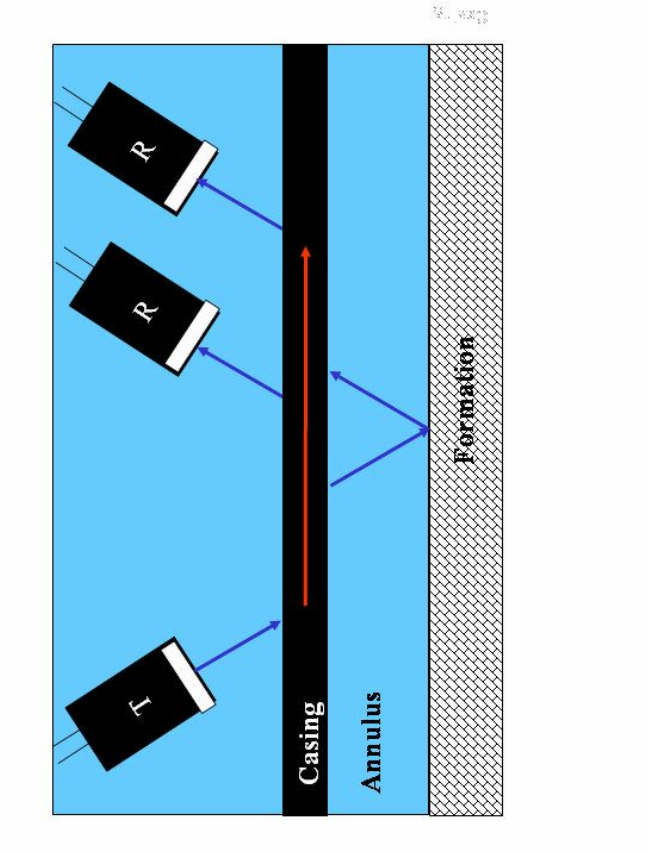

Fig.2 Pitch catch configuration used to transmit and receiver the flexural wave packets.

3 Flexural mode with cement

When the fluid behind casing is replaced by cement, the dispersion and attenuation curves are modified. Cement used in oilfield operations exhibits a variety of properties, either due to their formulations, or due to contamination with fluids encountered during their placement. However, typical values are listed in Table 1. The Poisson ratio for both cements is set at 0.30, as this value was experimentally demonstrated to be typical.

	Density kg/m3	Vp m/s	Vs m/s
Water	1000	1500	0
Steel	7800	5930	3250
Slow cement	1800	2600	1390
Fast cement	1800	3500	1870

Table 1 Materials acoustic properties.

3.1 Slow cement

The material designated as slow cement has a compressional velocity which intersects the expected flexural mode velocity. The mode search (Fig.3) shows that the phase velocity dispersion curve is split into 2 branches, with a small frequency domain around 200 kHz where 2 modes actually coexist. For the low frequency branch, the group velocity is slightly reduced compared to the fluid loaded case of Fig.1. The attenuation of the high frequency branch displays a significant increase compared to the fluid loaded case (140 dB/m versus 60 dB/m).

Full waveforms corresponding to the geometry of Fig.2 and one of the receivers have been simulated with a forward analytical model [5]. This model includes the finite size of the transducers apertures and their respective positions, and the different layers thicknesses and acoustic properties as listed in Table 1. The formation properties are assumed to be those of steel. The annulus thickness is fixed at 25 mm. Fig.4 display the results for different annulus materials. The bottom waveform is related to the liquid filled annulus, where the first event at 120 µs is the casing arrival, while the second event at 180 µs is the formation reflection, followed by multiples.

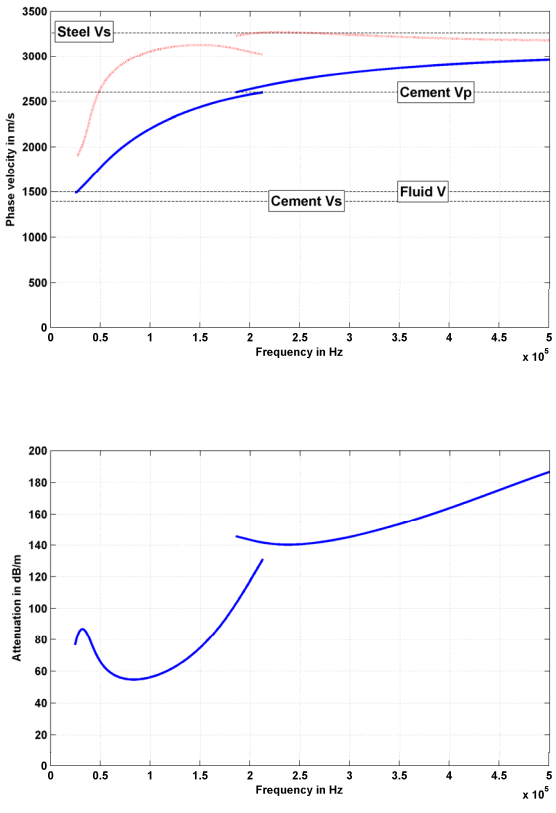

Fig.3 Dispersion and attenuation of a 8 mm steel plate with water on one side and slow cement on the other side.

The waveform with annulus filled with a slow cement exhibits a casing arrival which is both strongly reduced in amplitude and distorted. The low amplitude is a consequence of the high attenuation, and the distortion is the result of the coexistence of the 2 modes, the earlier high frequency one being followed by the low frequency, lower group velocity one. The events located after the casing arrival (after 140 µs) are reflection from the cement to formation interface. The high frequency branch phase velocity is faster than both compressional and shear velocities in cement, and thus radiates both waves in the annulus. The low frequency branch can only radiate shear wave in the annulus. The result is a succession of echoes corresponding to the propagation of compressional (PP), shear (SS) or mixed compressional and shear (SP or PS) waves. In addition, multiples are also present.

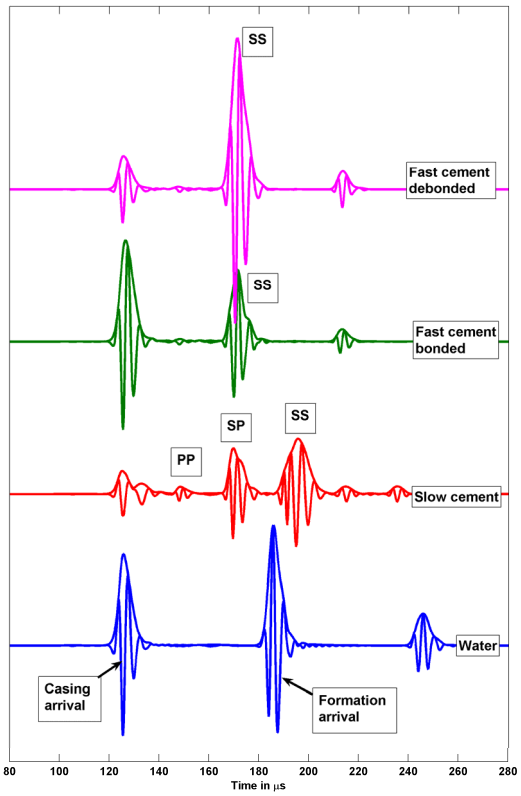

Fig.4 Simulated waveforms for different annulus materials. From bottom to top: Water, slow and fast cement and debonded fast cement.

3.2 Fast cement

When the cement compressional velocity increases beyond the flexural velocity, then it does not intersect the flexural mode dispersion curve (Fig.5). A small discontinuity is observed when the cement shear velocity crosses the dispersion. However, because cement shear velocity cannot exceed 2000 m/s, this discontinuity is well below 100 kHz and outside the frequency range of operation. The group velocity is back to values which are very close to what is noted for the fluid loaded case. The attenuation is now significantly smaller (40 dB/m) than for both the slow cement case and the water case.

On the received waveform (Fig.4) the casing arrival is larger than for the fluid loaded case. This lower attenuation

is actually related to the absence of radiation of compressional wave in the annulus. The only reflected event labelled SS at 160 µs is indeed a shear wave reflected at the formation boundary.

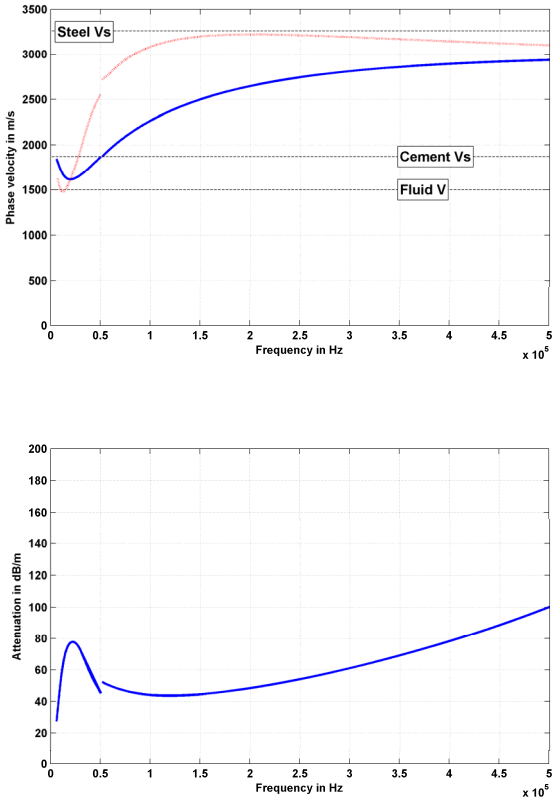

Fig.5 Dispersion and attenuation of a 8 mm steel plate with water on one side and fast cement on the other side.

3.3 Debonded cement

Debonded cement presents an interesting case relevant to field data. In field operations, debonding frequently occurs after thermal or pressure stresses, for example when the density of the fluid filling the pipe is reduced after cement setting. The dispersion and attenuation curves of a debonded fast cement are given in Fig. 6. Debonding is modeled with the inclusion of a thin (10 µm) water layer between the casing and the cement. Similar results would be obtained with a slip boundary conditions at the steel/cement interface.

Although the phase and group velocities are not significantly affected, a large increase in attenuation (from 40 to 110 dB/m) is noted following the lack of shear coupling between steel and cement. This effect is also seen on the waveform (Fig.4 top) which exhibits a strong reduction in amplitude for the casing arrival. The increase in shear radiation is also seen on the larger amplitude of the reflected shear formation arrival. It is thus paradoxical to see that a break in the shear stress coupling between the 2 solids results in an increase of the shear wave radiating into cement.

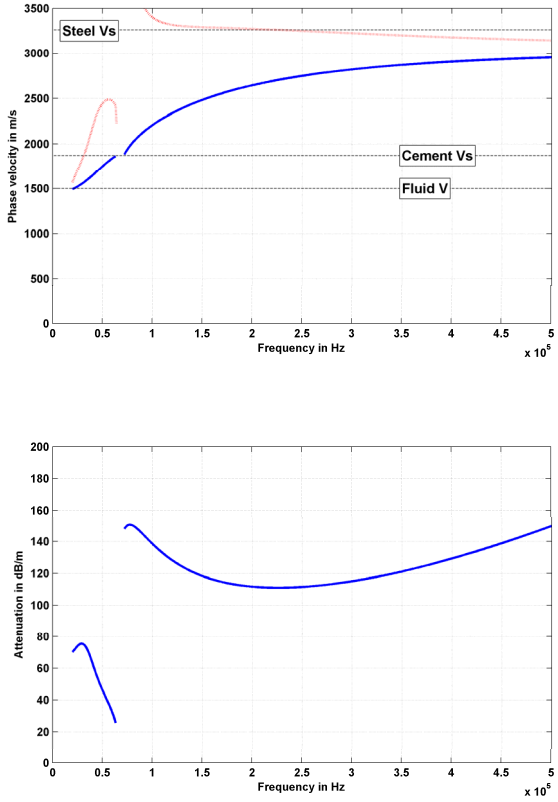

Fig.6 Dispersion and attenuation of a 8 mm steel plate with water on one side and debonded fast cement on the other side.

This effect is not seen with slow cement. Rather than plotting the full dispersion curves for the slow cement, Fig. 7 gives the modal attenuation at 200 kHz as a function of cement impedance, computed as the product of the density by compressional velocity. The density is fixed at 1800 kg /m3, and the Poisson ratio at 0.30. The first curve is for a perfect bond between steel and cement, while the second one is for the debonded case.

For the bonded case, the attenuation starts by increasing approximately linearly with the cement impedance, which can be extracted from its measurement. This attenuation peaks when the cement compressional velocity reaches 2600 m/s (or an acoustic impedance of 4.7 MRayls), yielding maximum sensitivity in the intermediate range where contrast between fluid and solid is rather low. Below this threshold, the flexural wave radiates both compressional and shear waves into the annulus. Above the threshold, the attenuation rapidly decreases, eventually to very low values. Shear wave only is radiated in the annulus since the flexural mode is beyond evanescence for compressional wave. The threshold corresponds to the switching from the high frequency high attenuation branch toward the low frequency low attenuation branch. .

For debonded cement, the attenuation shows a similar trend below evanescence, with a linear increase with cement impedance and only a slight reduction compared to the bonded case. However, above evanescence, cement debonding produces a completely different behaviour, with

again a linear increase in attenuation. High impedance debonded cement (6-8 MRayls) appear like bonded moderate impedance (3-4.5 MRayls) solids.

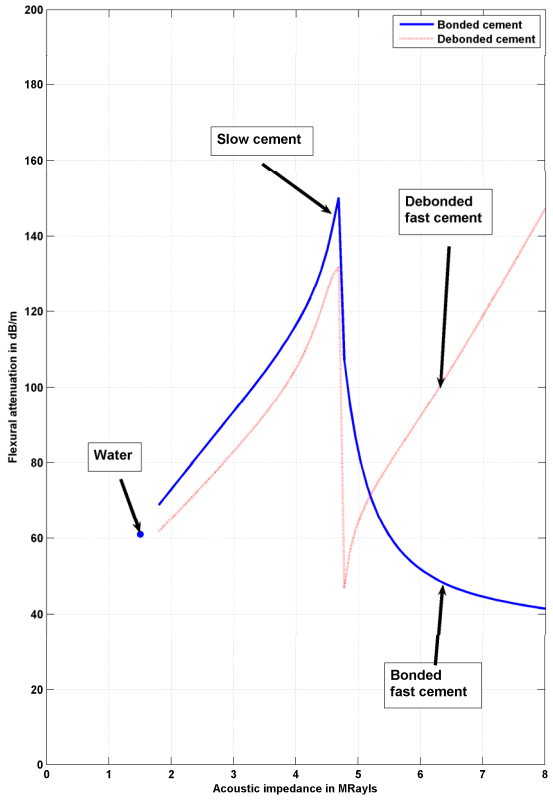

Fig.7 Flexural mode attenuation of a 8 mm steel plate at 200 kHz as a function of cement impedance.

4 Conclusion

We have described the main characteristics of the pipe flexural mode dispersion and attenuation curves. A broad maximum of the group velocity with frequency affords opportunity to make easy and accurate time and amplitude measurements on broadband compact echoes. The effect of cement in the annulus depends upon its mechanical properties: The attenuation first increases linearly with its acoustic impedance and peaks when the cement compressional velocity is matching the flexural phase velocity. Beyond this point, the attenuation sharply drops down to very low values for high impedance cement. Introducing a slip boundary condition at the steel/cement interface (debonded cement) has a minor effect on low impedance cement and a drastic effect on high impedance cement, with a large increase in attenuation.

These effects have been matched with features of simulated time waveforms, and provide explanations for experimentally observed field data. In actual field operations, the flexural data such as attenuation or formation arrival time, are merged with the data obtained from the thickness resonance mode. The result of this combination is an enhanced diagnostic of the annulus condition, extending the depth of investigation

Acknowledgments

The author thanks S.Zeroug for providing the modeling code used for simulating the full waveforms.

References

[1] A.J.Hayman, P.Parent, P.Cheung,, and P.Verges, "Improved borehole imaging by ultrasonics", *Paper SPE 28440, 69th SPE Annual Technical Conference and Exhibition, New Orleans, LA* (1994).

[2] S.Zeroug and B.Froelich,"Ultrasonic leaky-Lamb wave imaging through a highly contrasting layer", *Proc. IEEE Ultrason. Symp.*, November 2003, 794-798.

[3] R. van Kuijk, S.Zeroug, B.Froelich, M.Allouche, S.Bose, D.Miller, J.-L. Le Calvez, V.Schoepf, A.Pagnin, "A novel ultrasonic cased-hole imager for enhanced cement evaluation", *Paper SPE 10546, International Petroleum Technology Conference*, September 2005.

[4] M.J.S.Lowe, "Matrix techniques for modelling ultrasonic waves in multilayered media ", *IEEE Trans. Ultrason. Ferroelectr. Freq. Contr*, 42 (1995) pp 525-542.

[5] S.Zeroug, "Forward modeling for leaky Lamb-wave imaging through a highly contrasting steel cylindrical layer", *Proc. IEEE Ultrason. Symp.*, August 2004, 672 – 675.